Journal of Alloys and Compounds 495 (2010) 275–279

Contents lists available at ScienceDirect

Journal of Alloys and Compounds

journal homepage: www.elsevier.com/locate/jallcom

Effect of thermal treatment on the structure and optical properties of biomimic hierarchical ZnO column arrays

Mei Yang[a,b], Zhongbing Huang[a], Guangfu Yin[a], Xiaoming Liao[a,*], Yadong Yao[a], Yunqing Kang[a], Jianwen Gu[c,**]

[a] College of Materials Science and Engineering, Sichuan University, Chengdu 610064, China
[b] College of Materials and Chemistry & Chemical Engineering, Chengdu University of Technology, Chengdu 610059, China
[c] Chengdu Military General Hospital, Chengdu 610083, China

ARTICLE INFO

Article history:
Received 24 November 2009
Received in revised form 29 January 2010
Accepted 5 February 2010
Available online 12 February 2010

Keywords:
Thermal treatment
Hierarchical
ZnO column arrays
Optical properties

ABSTRACT

In order to study the effect of thermal treatment on the structure and optical properties of biomimic hierarchical ZnO column arrays, the as-grown biomimic hierarchical ZnO column arrays were annealed in air from 200 to 650 °C, and the change of their hierarchical structure was observed by the high-resolution transmission electronic microscopy image. The UV–vis spectra exhibited an interesting change of the structure with different annealing temperatures. Photoluminescence intensity of annealed biomimic arrays was increased at about 520 nm. The mechanism of visible emission was also discussed.

1. Introduction

ZnO, a typical II–VI group compound semiconductor, is an excellent electronic and photonic material due to the wide direct band gap (3.37 eV) at room temperature and large exciton binding energy (60 meV) which is much higher than that of ZnSe (20 meV) and GaN (21 meV) [1]. In recent years, it has attracted much attention because of the increasing need for short-wavelength photonic devices, electronic devices [2–4], light-emitting diodes [5], photodetectors [6], and so on. Moreover, its ultraviolet and blue emission has been drawing considerable attention recently [7–10].

Because the annealing treatment has significant influence on the structure and the photoluminescence (PL) of ZnO films, many studies [11–19] have researched the relationship between the annealing temperature and PL property of ZnO thin films. Sun et al. [11] studied the influence of annealing atmosphere on the electrical and optical properties of the deposited ZnO thin films. Ran et al. [16] reported that the PL intensity of ZnO films was decreased when annealing temperature exceeded a certain temperature. Study of Choppali et al. revealed that there was an increase of grain size and texture coefficient along the *c*-axis for the ZnO thin films with the increase of annealing temperature [18]. Some groups also have researched the biomimetic array of ZnO nanorods through multi-step or long reaction time [19,20]. However, the direct fabrication of large-scale arrays of the hierarchical ZnO columns with controlled crystalline structure remains a significant challenge.

We have successfully prepared biomimic hierarchical ZnO column arrays by sol–gel method through adding dimercaptosuccinic acid (DMSA), and they possess layer-by-layer nano-structure and PL property, which are similar to those of biogenic calcium carbonates [21]. Their layer-by-layer bonding depends on DMSA molecules. As we have known, dimercaptosuccinic acid is a chelator, which can be bound to the metals. The connection between DMSA and ZnO was zinc ions and mercapto sulfur atom. Briefly, the bonds of S–Zn will form because of the bond of SH cleaves and the strong affinity between S and Zn. For the thiol groups of DMSA linked with ZnO may inhibit the further growth of ZnO along (0 0 1) direction, the thiol groups of DMSA between ZnO sheets can be connected through the condensation of two SH groups. Sequentially, the unusually oriented column-like structures of ZnO sheets can be formed through orderly stacking of ZnO sheets, which are directly relative to the function of DMSA [21]. The detailed explanation of the mechanism for the layer-by-layer growth of ZnO by the addition of DMSA was described in our previous paper [21]. However, effects of the thermal treatment on the layer-by-layer structure and optical properties of biomimic hierarchical ZnO column structures still remain open questions. In this work, we studied the change of the structure and the optical properties of biomimic hierarchical ZnO

* Corresponding author. Tel.: +86 28 85413003.
** Corresponding author. Tel.: +86 28 86570361.
E-mail addresses: sherman_xm@163.com (X. Liao), gujianwen5000@yahoo.com.cn (J. Gu).

0925-8388/$ – see front matter © 2010 Elsevier B.V. All rights reserved.
doi:10.1016/j.jallcom.2010.02.016

column arrays after annealed at 200–650 °C in air, and discussed the mechanism of the changed optical properties of the annealed biomimic ZnO column arrays.

2. Materials and methods

2.1. Materials

Analytic grade hexamethylene tetramine, zinc nitrate hexahydrate were purchased from Chengdu Kelong Chemical Co. Ltd. (China). Dimercaptosuccinic acid (99%) was obtained from Acros, USA.

2.2. Preparation of biomimic hierarchical ZnO column arrays

The biomimic hierarchical ZnO column arrays were prepared on common glass substrates. The cleaned glass slides were immersed in the solution containing an equimolar zinc nitrate-6-hydrate [$Zn(NO_3)_2{\cdot}6H_2O$] and hexamethylenetetramine [HMT] (0.05 M) for 5 min, and then heated at 500 °C for 10 min in a muffle furnace. The coating process was done three times to ensure complete and uniform coverage of ZnO seeds on the substrates. The prepared ZnO seed layers were used as the buffered layers for the growth of biomimic ZnO column arrays. Subsequently, the glass slides with buffered layers were placed vertically in a solution containing equimolar $Zn(NO_3)_2{\cdot}6H_2O$ and HMT (0.025 M), and reacted at 80 °C, then DMSA with a concentration of 0.0025 M was added into the above aqueous solution after reactions had been for 5 h, and continued to react at 80 °C for 12 h. After that, the glass slides were removed from the aqueous solution and rinsed with deionized water several times. Finally, the glass slides were dried at room temperature.

2.3. Heat treatment of biomimic hierarchical ZnO column arrays

The as-prepared biomimic hierarchical ZnO column arrays were annealed at 200–650 °C in air for 60 min and subsequently cooled to the room temperature.

2.4. Characterization

The morphology of the annealed hierarchical ZnO column arrays was characterized by scanning electron microscopy (SEM, JSM-5900LV, Japan). The crystalline structure of the samples was analyzed using X-ray diffraction (XRD, X'Pert, Holand) with Cu Kα radiation. The diverse photoluminescence characteristics of hierarchical ZnO columns array annealed at various temperatures were investigated through the PL measurement (F-7000, Hitachi) with Xe laser at room temperature, and ultraviolet–visible (UV–vis) spectra performed by U-3010 spectrophotometer. The crystal lattice of the annealed ZnO column at 600 °C for 1 h was characterized by high-resolution transmission electronic microscopy (HRTEM, JEM-2100, Japan) and accompanying selected area electron diffraction (SAED). Differential scanning calorimeters (DSC) and thermogravimetry (TG) were carried out with TG/SDTA851^e analyzer by METTLER-TOLEDO Co. of Switzerland. 10 mg of the powder was placed into an alumina vessel and heated at a rate of 2.5 °C/min up to 700 °C in air.

3. Results and discussion

3.1. Structure and morphology

Fig. 1 shows the morphologies of unannealed and annealed biomimic hierarchical ZnO column arrays. In Fig. 1a, each column contains lots of hexagonal ZnO wafers with a diameter of ~0.8 μm. The cross-section image in the inset of Fig. 1a shows that the thickness of ZnO column array is about 1 μm, and that the columns almost grow vertically to the substrate. When biomimic hierarchical ZnO column arrays are annealed at 200 °C for 1 h, the hierarchical structure can remain, and the expected surface becomes less smooth compared with unannealed ZnO columns (Fig. 1b). The surface becomes rough when the sample is annealed at 400 °C, and the diameter of hexagonal ZnO wafers has decreased to ~200 nm (shown in Fig. 1c). A column with about 1 μm length on the ZnO film (marked by an arrow in Fig. 1c) indicates that the thickness of film still remains at about 1 μm after annealing at 400 °C. Fig. 1d is the morphology of the sample after annealing at 650 °C, showing that the thin wafers in column are fused together, and morphology of ZnO column arrays has deteriorated. The change of morphology should result from the decomposition of DMSA, which

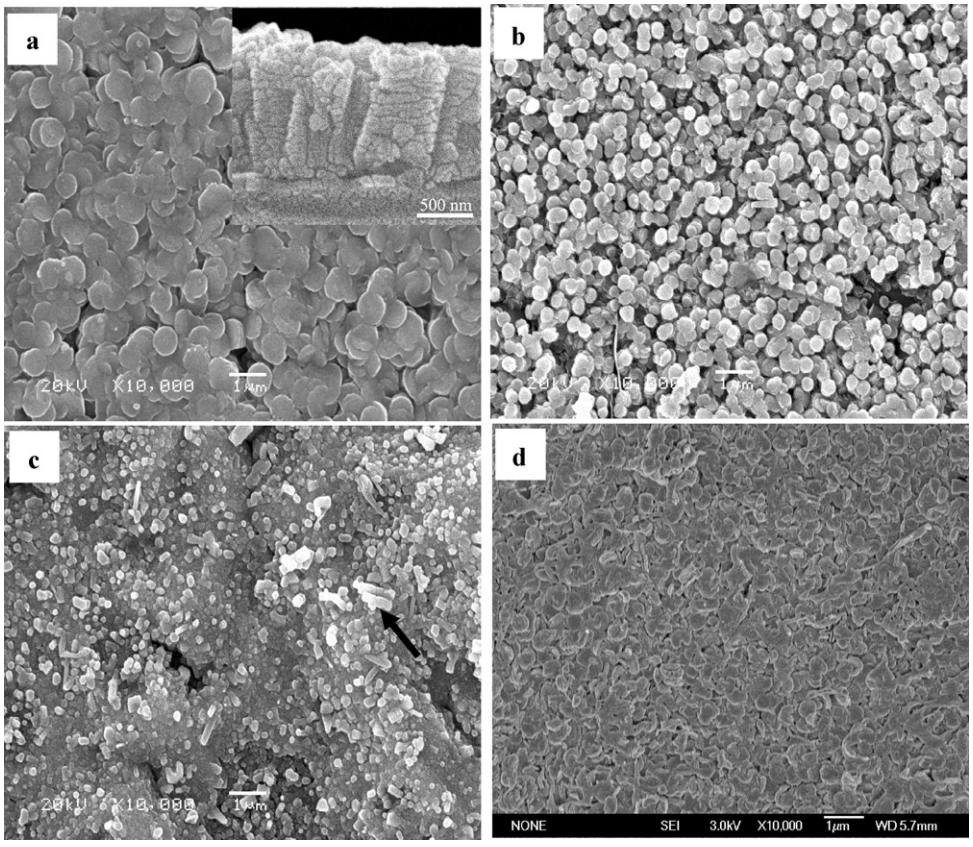

Fig. 1. SEM images of (a) unannealed biomimic hierarchical ZnO column arrays, inset is the cross-section image of the sample, and annealed biomimic ZnO column arrays at (b) 200 °C; (c) 400 °C and (d) 650 °C.

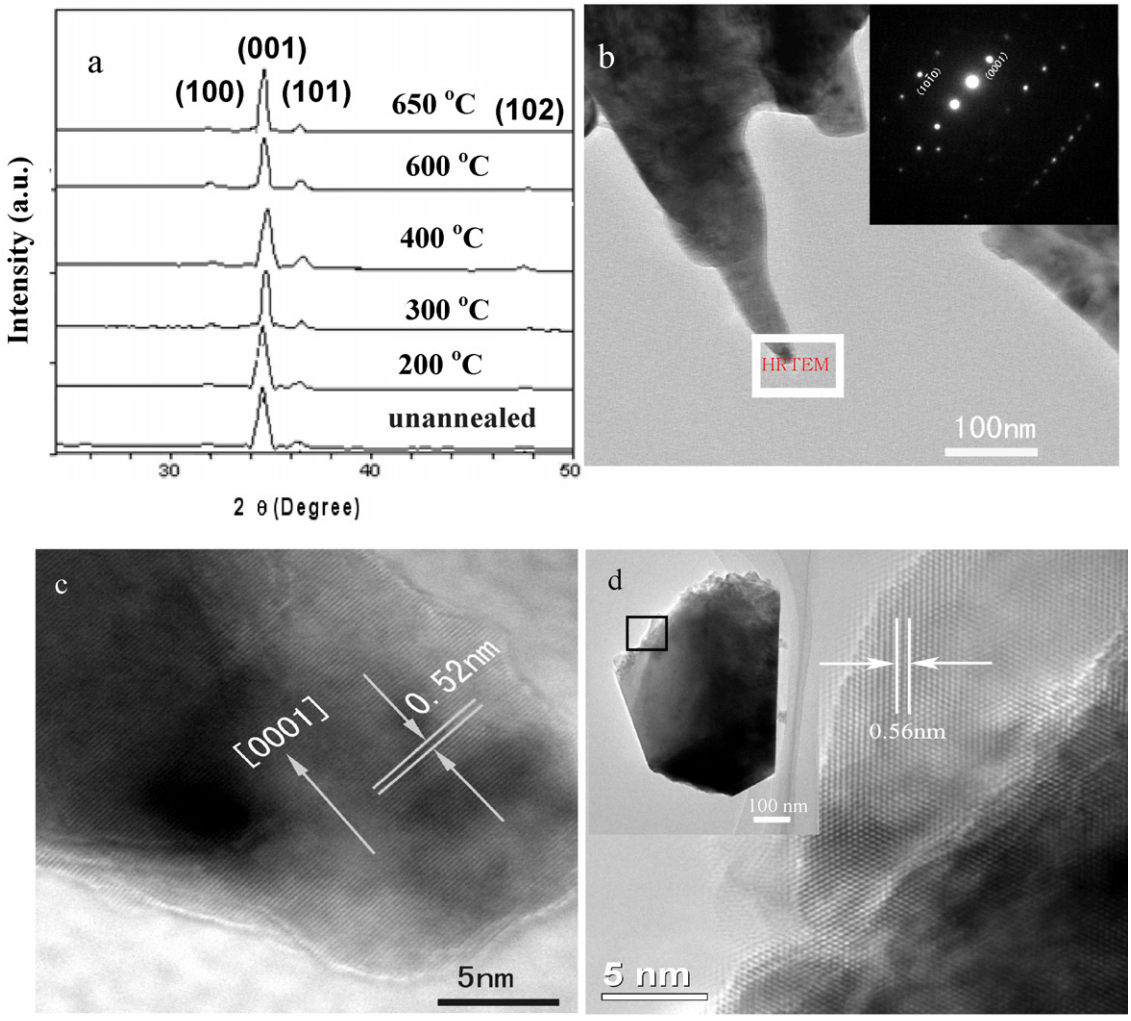

Fig. 2. (a) XRD patterns of samples treated under different conditions, (b) TEM image of ZnO column annealed at 600 °C for 1 h, inset is SAED pattern corresponding to the small frame area marked, and (c) the corresponding HRTEM image; (d) HRTEM image of an unannealed ZnO column, corresponding to the small square area marked in inset.

connects with two ZnO ultrathin sheets (shown in our previous paper [21]).

Fig. 2a shows the XRD patterns of the samples treated under different conditions. All diffraction peaks can be indexed to the wurtzite phase of ZnO (Joint Committee on Powder Diffraction Standards (JCPDS) Card No. 89-1397). It shows that the column arrays grow along [0 0 1] direction after annealing treatment and the intensity of (0 0 1) peak is the strongest in ZnO characteristic peaks. Moreover, the change of (0 0 1) peak intensity could be observed from 200 to 650 °C. The XRD patterns also reveal that ZnO column arrays exist a preferred (0 0 1) orientation, which can be attributed to the fact that the surface free energy of ZnO (0 0 1) plane is minimum at the growth stage [15]. Fig. 2b presents a TEM image for the tip of a typical ZnO column annealed at 600 °C for 1 h. The corresponding SAED pattern (the inset in Fig. 2b) indicates the single crystalline nature of the annealed ZnO column. HRTEM image in Fig. 2c shows the 2.6 Å {0 0 1} lattice fringe parallel to the basal plane, which is taken from the rectangle region of the rod in Fig. 2b. It provides further confirmation that the columns are growing along the [0 0 1] direction. Some layer-by-layer structures are also observed in Fig. 2c. Fig. 2d is HRTEM image of unannealed ZnO column corresponding to the small square area marked in inset of its TEM image, and it shows clear layer-by-layer structure. These results indicate that the hierarchical layer-by-layer structure of ZnO rod could remain after annealing.

In order to confirm the effect of annealing treatment on ZnO columns, TG/DSC analysis in air was carried out. Fig. 3 shows the TG/DSC curves of an unannealed ZnO column sample. Moderate weight loss for the sample up to about 200 °C is attributed to the release of adsorbing water on the surface. The endothermic events

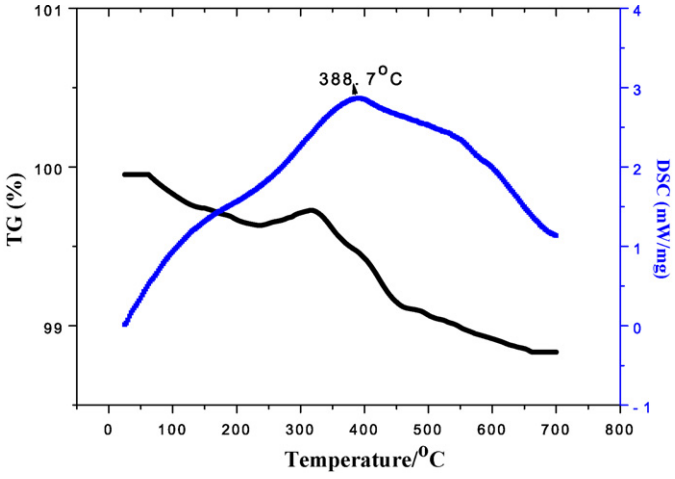

Fig. 3. TG/DSC curves of unannealed biomimic hierarchical ZnO column arrays.

with large weight loss of about 2% around 388 °C could result from the thermal decomposition and carbonization of DMSA, revealing that there is about 2 wt% of organic component (DMSA) in the unannealed ZnO column sample. The continuous decrease of DSC curve after 600 °C indicates that the oxidation of these carbonizations also continues to occur. The thermal decomposition and carbonization of DMSA, which could exist among the (0 0 1) planes in the unannealed ZnO column sample, resulted in the slight change of the lattice spacing of the sample from 0.56 nm of the unannealed into 0.52 nm of the annealed.

3.2. Optical properties

Fig. 4 shows the UV-reflectance spectra of biomimic hierarchical ZnO column arrays annealed at different temperatures. The reflectance below 375 nm is rather weak due to the band gap light absorption [22]. However, an abrupt increase in reflectance at ~425 nm is observed for all samples. The reflectance of hierarchical ZnO column arrays is decreased gradually with the increase of annealing temperatures from 200 to 400 °C, which results from sintering of DMSA leftover and the destroyed smooth facet of hierarchical ZnO column arrays during heat treatment, which are corresponding with the results of TG/DSC and SEM images (Figs. 3 and 1). On the other hand, the reflectance is markedly enhanced as the temperature is increased to 600 °C, it may be due to the conjunction of the thin wafers in column, which results in the ZnO increasing density on the substrate as a whole. This is corresponding with the results of SEM images.

Fig. 5 is the PL spectra of the biomimic samples annealed at different temperatures. It is obvious that two peaks of 395 nm and 420 nm in these PL curves are joined together, which is resulted from the change of the intrinsic structures and zinc vacancy, respectively. Many studies had indicated that the UV emission might be due to the band-to-band transition and the free exciton recombination [23,24]. In this case, the main peak results from the confusion of two peaks of 395–420 nm after annealing. From Fig. 5, it could be observed that the increased intensity of the peak at 420 nm is more than that of the peak at 395 nm after annealing. In addition to the emission in UV region, the change of visible emission can be observed and two main peaks can be identified at 465 nm and 520 nm. The intensity of peaks at 465 nm and 520 nm is all increased, which also indicates the change of defects in ZnO. These phenomena could be explained as follows.

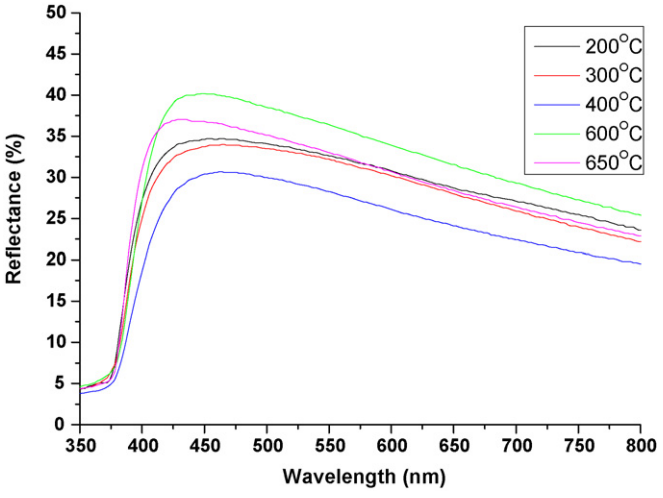

Fig. 4. Reflectance spectra of the biomimic hierarchical ZnO column arrays annealed at different temperatures.

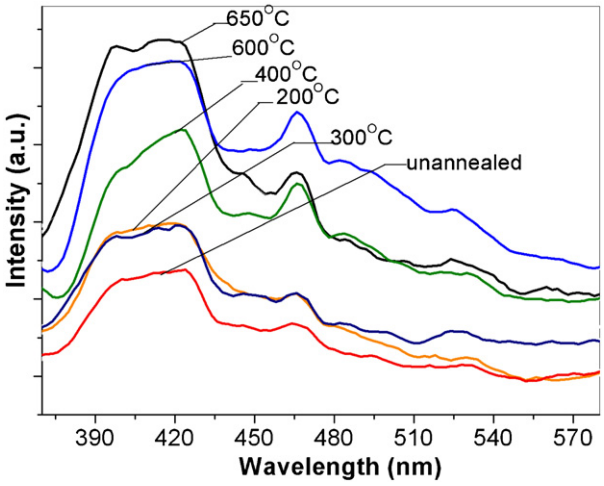

Fig. 5. PL spectra of the samples annealed at different temperatures.

However, it is well known that ZnO easily produces intrinsic defects such as interstitial zinc (Zn_i) and oxygen vacancy (V_O). These defects will affect the photoluminescence behavior of ZnO in different ways [25]. Fig. 6 is the sketch of the defect's levels in ZnO. The energy interval from the bottom of the valence band to the Zn_i level (2.9 eV) is exactly consistent with the energy of the UV emission observed in our experiment. As shown in Fig. 5, the increased intensity of UV emission results from the decrease of organic leftover due to oxidation. Because the radius of Zn^{2+} is smaller than that of O^{2-}, Zn_i may exist in crystalline after they were annealed. As a result, Zn_i provides a great lot of electrons for conduction band that could produce UV emission through the formation of exciton with valence band cavity [1]. Although the annealing treatment in air maybe make O enter into the crystal lattice and decrease oxygen vacancy with the increase of the annealing temperature [26], oxygen vacancy could be inevitably increased because lots of organic molecules were removed during the annealing treatment.

Besides the UV emission in PL spectra, visible emission is observed around ~520 nm. The work of Vanheusden et al. [27] assigned green emission around ~520 nm to the transition between the photoexcited holes and singly ionized oxygen vacancy. Because the center energy of the green peak, 2.40 eV, is smaller than the band gap energy of ZnO film, 3.3 eV, the green emission must be related to a local level in band gap. Thus, the intensity variation of the green emission might result from the variation of the intrinsic defects in ZnO columns, such as zinc vacancy V_{Zn}, oxygen vacancy V_O, interstitial zinc Zn_i, interstitial oxygen O_i, and antisite oxygen O_{Zn}. It can be seen from Fig. 6 that the energy interval from the valence band edge to the oxygen vacancy V_O (2.40 eV) is consistent with the energy of the green emission observed in the experiment.

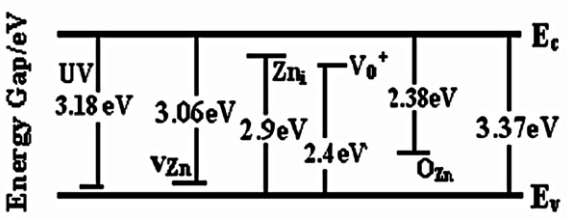

Fig. 6. A schematic diagram of the defect state levels for ZnO.

4. Conclusions

In summary, we have demonstrated the changes of structure and optical properties of biomimic hierarchical ZnO column arrays annealed at different temperatures. HRTEM images and XRD results display that the typical structure of ZnO remains after annealing. PL spectra suggest that the central emission of the annealed hierarchical ZnO column samples transfers from 395 nm to 420 nm after annealing. The mechanism of the increasing photoluminescence intensity of ZnO column arrays at about 520 nm needs to be further investigated in future. Moreover, the reflectance spectra property exhibits an interesting variation of the morphology with the different annealing temperatures.

Acknowledgements

This work has been supported by the National Natural Science Foundation of China (Project Nos. 60871062 and 50873066). The supports of Sichuan Province through a Science Fund for Distinguished Young Scholars of Sichuan Province (08ZQ026-007 and 07ZQ026-118) and Key Technologies Research and Development Program of Sichuan Province (2008SZ0021 and 2006Z08-001-1) are also acknowledged with gratitude. This work was also supported by the Specialized Research Fund for the Doctoral Program of Higher Education from Ministry of Education of China (20070610131) and the 11th Five-year Program for Medicine and Health Science Research of Chinese PLA (08z011). We thank Analytical & Testing Center, Sichuan University for the assistance with the microscopy work. The authors would also like to thank Mrs. Hui Wang of Analytical & Testing Center, Sichuan University for her support and encouragement.

References

[1] B.X. Lin, Z.X. Fu, Y.B. Jia, Appl. Phys. Lett. 79 (2001) 943.
[2] A. Sasaki, W. Hara, A. Matsuda, N. Tateda, S. Otaka, S. Akiba, Appl. Phys. Lett. 86 (2005) 231911.
[3] T. Makino, Y. Segawa, A. Tsukazaki, A. Ohtomo, M. Kawasaki, Appl. Phys. Lett. 87 (2005) 022101.
[4] S. Deka, P.A. Joy, Appl. Phys. Lett. 89 (2006) 032508.
[5] R. Könenkamp, R.C. Word, C. Schlegel, Appl. Phys. Lett. 85 (2004) 6004.
[6] C.H. Chen, S.J. Chang, Y.K. Su, G.C. Chi, J.Y. Chi, C.A. Chang, J.K. Sheu, J.F. Chen, Photon. Technol. Lett. 13 (2001) 848.
[7] D.M. Bagnall, Y.F. Chen, Z. Zhu, T. Yao, S. Koyama, M.Y. Shen, T. Goto, Appl. Phys. Lett. 70 (1997) 2230.
[8] H. Cao, Y.G. Zhao, S.T. Ho, E.W. Seeling, Q.H. Wang, R.P.H. Chang, Phys. Rev. Lett. 82 (1999) 2278.
[9] P. Zu, Z.K. Tang, G.K.L. Wong, M. Kawasaki, A. Ohtomo, H. Koinuma, Y. Segawa, Solid State Commun. 103 (1997) 456.
[10] S.L. Cho, J. Ma, Y.K. Kim, Y. Sun, G.K.L. Wang, J.B. Ketterson, Appl. Phys. Lett. 75 (1999) 2761.
[11] J.C. Sun, T.P. Yang, G.T. Du, H.W. Liang, J.M. Bian, L.Z. Hu, Appl. Surf. Sci. 253 (2006) 2066.
[12] L.E. Greene, M. Law, J. Goldberger, F. Kim, J.C. Johnson, Y.F. Zhang, R.J. Saykally, P.D. Yang, Angew. Chem. Int. Ed. 42 (2003) 3031.
[13] B. Marí, M. Mollar, A. Mechkour, B. Hartiti, M. Perales, J. Cembrero, Microelectron. J. 35 (2004) 79.
[14] Y.J. Kim, H.J. Kim, Mater. Lett. 41 (1999) 159.
[15] P.T. Hsieh, Y.C. Chen, K.S. Kao, M.S. Lee, C.C. Cheng, J. Eur. Ceram. Soc. 27 (2007) 3815.
[16] F.Y. Ran, L. Miao, S. Tanemura, M. Tanemura, Y.G. Cao, S. Tanaka, N. Shibata, Mater. Sci. Eng. B 148 (2008) 35.
[17] M. Jung, J. Lee, S. Park, H. Kim, J. Chang, J. Cryst. Growth 283 (2005) 384.
[18] U. Choppali, B.P. Gorman, Opt. Mater. 31 (2008) 143.
[19] R.T. Zhengrong, A.V. James, L. Jun, M. Bonnie, J.M. Matthew, J. Am. Chem. Soc. 124 (2002) 12954.
[20] Y. Shu, S. Tsugio, J. Mater. Chem. 15 (2005) 4584.
[21] M. Yang, G.F. Yin, Z.B. Huang, Y.Q. Kang, X.M. Liao, H. Wang, Cryst. Growth Des. 9 (2009) 707.
[22] M.S. Wang, E.J. Kim, H.H. Sung, P. Chinho, K.K. Koo, Cryst. Growth Des. 8 (2008) 501.
[23] Y. Zhang, B.X. Lin, Z.X. Fu, C.H. Liu, W. Han, Opt. Mater. 28 (2006) 1192.
[24] S.Y. Kuo, W.C. Chen, C.P. Cheng, Superlattice Microstruct. 39 (2006) 162.
[25] Y.S. Park, C.W. Litton, T.C. Collins, D.C. Reynolds, Phys. Rev. 143 (1966) 512.
[26] J. Xu, Z.Y. Zhang, Y. Zhang, B.X. Lin, Z.X. Fu, Chin. Phys. Lett. 22 (2005) 2031.
[27] K. Vanheusden, W.L. Warren, C.H. Seager, D.R. Tallant, J.A. Voigt, B.E. Gnade, J. Appl. Phys. 79 (1996) 7983.